The contribution of active hair-bundle motility to nonlinear amplification in the mammalian cochlea

Fumiaki Nin, Tobias Reichenbach, Jonathan A. N. Fisher, and A. J. Hudspeth*

Howard Hughes Medical Institute and Laboratory of Sensory Neuroscience, The Rockefeller University, 1230 York Avenue, New York, New York 10065, USA

The cochlea's high sensitivity stems from the active process of outer hair cells, which possess two force-generating mechanisms: active hair-bundle motility elicited by Ca^{2+} influx and somatic motility mediated by the voltage-sensitive protein prestin. Although interference with prestin has demonstrated a role for somatic motility in the active process, it remains unclear whether hair-bundle motility contributes *in vivo*. We selectively perturbed the two mechanisms by infusing substances into the endolymph or perilymph of the chinchilla's cochlea, then used scanning laser interferometry to measure vibrations of the basilar membrane. Blocking somatic motility, damaging the tip links of hair bundles, or depolarizing hair cells eliminated amplification. While reducing amplification to a lesser degree, pharmacological perturbation of active hair-bundle motility diminished or eliminated the nonlinear compression underlying the broad dynamic range associated with normal hearing. The results suggest that active hair-bundle motility plays a significant role in the amplification and compressive nonlinearity of the cochlea.

\body

The sense of hearing excels in several ways. Human hearing spans the enormous frequency range from 20 Hz to 20 kHz, yet we can distinguish frequencies that are only 0.2 % apart. This interval is well below a semitone in Western music, which represents about 6 % in frequency. Moreover, humans can perceive trillionfold differences in sound intensity, yet the faintest detectable sounds vibrate the tympanic membrane by only 10 pm. These extraordinary features ensue from an active process that provides tuned mechanical amplification of weak signals in the mammalian cochlea. Stimulation with a pure tone elicits a wave of basilar-membrane motion that travels apically and peaks at a frequency-dependent position: high frequencies evoke a maximal response near the cochlear base and progressively lower frequencies at successively more apical positions[1-4]. As a traveling wave advances, the active process of outer hair cells continuously adds energy to the vibration to counter the dissipative effect of viscosity[5-7].

The molecular basis of the active process remains unclear. The outer hair cells of mammals exhibit a unique form of mechanical activity: their cell bodies change in length when the membrane potential is altered[8,9]. This somatic motility or electromotility is produced by the membrane protein prestin, which undergoes conformational changes upon alteration of the membrane potential[10]. Several experimental studies demonstrate that somatic motility is required for the active process in the cochlea. Transgenic mice in which prestin has been incapacitated or eliminated display severely elevated hearing thresholds[11-14]. In wild-type animals, targeted inactivation of prestin over cochlear segments near a traveling wave's peak dramatically reduces the gain [15].

The mechanoreceptive hair bundles of many vertebrates are also mechanically active. Bundles can oscillate spontaneously in the absence of external forcing and perform mechanical work to amplify inputs; their response is frequency-tuned and compressively nonlinear[16,17]. Although active hair-bundle motility has been studied predominantly in the hair cells of amphibians and reptiles[18,19], *in vitro* studies demonstrate that it contributes to the active process of the mammalian cochlea as well[20-23]. It has not heretofore been possible, however, to

investigate the role of mammalian hair-bundle activity *in vivo*. Because mechanotransduction is required to elicit somatic motility, interfering with a hair bundle's operation usually affects somatic motility as well. It is accordingly difficult to isolate the contribution of active hair-bundle motility to the mammalian active process. To overcome this problem, we have developed an *in vivo* preparation of the chinchilla's cochlea that allows us to record sound-induced waves on the basilar membrane with a scanning laser interferometer. We have then studied the effects of pharmacological agents that interfere with hair-bundle activity while leaving mechanotransduction and somatic motility intact.

Results

Velocity and sensitivity of the traveling wave under control and anoxic conditions

By directing the beam of a scanning laser interferometer through a 0.5 mm window in the bony wall of the chinchilla's cochlea slightly apical to the round window, we measured the vibration velocity of the basilar membrane (Fig. 1a). For any particular sound-pressure level (SPL), the velocity under control conditions exceeded that after anoxia (Fig. 1b). Moreover, the traveling wave peaked more apically under control conditions than after anoxia. The extent of compressive nonlinearity was especially apparent in graphs of the sensitivity, which was calculated as the ratio of the velocity to the stimulus level (Fig. 1c). Low-level stimulation of a control cochlea evoked a narrow traveling-wave peak with a maximal sensitivity exceeding 10 $mm \cdot s^{-1} \cdot Pa^{-1}$, whereas the sensitivity after anoxia was at least an order of magnitude lower, typically 0.2 $mm \cdot s^{-1} \cdot Pa^{-1}$, and nearly independent of the stimulus level. All these characteristics are indicative of a robust cochlear active process with a gain of 50× or more.

Effect of blocking somatic motility and damaging tip links

We first conducted control experiments meant to confirm the effects of interference with somatic motility and mechanoelectrical transduction. While measuring traveling waves *in vivo*, we

exposed the cochlea to salicylate, which interacts with prestin and reduces somatic motility in outer hair cells[24] without any known effect on active hair-bundle motility. Fifteen minutes after the application of 3 mM salicylate to the perilymph, the sensitivity of the traveling wave decreased to the level characteristic of anoxia (Fig. 2a). This result was confirmed in three additional experiments. Similar effects have been observed previously after salicylate treatment or genetic perturbation of prestin[12,14,25].

We next iontophoresed into the endolymph the Ca^{2+} chelator BAPTA, which breaks tip links by lowering the Ca^{2+} concentration[25]. As the chelator diffused to the hair bundles over a period of 60 min, the basilar membrane's sensitivity in each of three experiments declined to the level characteristic of anoxia (Fig. 2b).

High-K^+ solution depolarizes hair cells, thereby decreasing the mechanoelectrical-transduction current, which depends on the difference between the endocochlear potential and the membrane potential of hair cells. Depolarization also impairs voltage-driven somatic motility. An elevated K^+ concentration should therefore disable both components of the active process and eliminate amplification. Within 15 min of its application in the perilymph, 150 mM KCl reduced the sensitivity in each of three preparations to the value after anoxia (Fig. 2c).

After each of these three control perturbations, the peak of the traveling wave shifted basally as observed under anoxia (Fig. 2a-c). These results together indicate that blocking either mechanoelectrical transduction or electromotility has the same effect as nonspecifically disrupting both components of the active process.

Effect of perturbing active hair-bundle motility

Although no specific blocker of active hair-bundle motility is known, several substances have been demonstrated to affect this process *in vitro*. Calcium ion has a pronounced effect on hair-bundle oscillations: increasing the Ca^{2+} concentration progressively accelerates bundle oscillations and lowers their magnitude[27]. Rp-adenosine 3′,5′-cyclic monophosphorothioate

(Rp-cAMPS), which is an inhibitor of cAMP-dependent protein kinase and thus of protein phosphorylation in hair cells, reduces the frequency of spontaneous oscillation *in vitro*[27]. In contrast, Sp-adenosine 3′,5′-cyclic monophosphorothioate (Sp-cAMPS), an activator of the same enzyme, increases the oscillation frequency; a related substance, 8-bromoadenosine 3′,5′-cyclic monophosphate (8-Br-cAMP), shifts the hair bundle's displacement-response relation[28]. Use of these compounds therefore permits manipulation of hair-bundle motility without damaging the mechanotransduction apparatus or directly affecting somatic motility.

In a total of four experiments, iontophoretic application of Ca^{2+} to the endolymph substantially decreased the traveling wave's sensitivity (Fig. 2d). A treated cochlea displayed greater sensitivity than an anoxic one, but its response was distinctly more linear than that of a control preparation.

Rp-cAMPS and 8-Br-cAMP had similar effects on the traveling wave; after exposure to either substance the sensitivity fell to about one-fifth the control value but remained fivefold that for anoxia (Fig. 2e,f). This result was observed four times for each substance. The traveling wave's peak shifted basally and the wave broadened in both instances. To confirm that the drugs did not interfere with prestin on the basolateral surfaces of the hair cells or with other cells in the organ of Corti, we also infused these substances into the perilymph; both treatments were without significant effect (Fig. S1).

In a linear system the phase of the traveling wave and the location of its peak are independent of the sound-pressure level. We observed this behavior after anoxia, blocking somatic motility, or breaking tip links (Fig. 2). Under control conditions, however, the phase and peak location showed a clear level dependence indicative of nonlinearity. The level dependence of both the phase and the peak position persisted after treatment with Ca^{2+}, Rp-cAMPS, or 8-Br-cAMP, confirming that some nonlinearity remained (Fig. 2d-f; Fig. S2).

By relating basilar-membrane sensitivity to the level of stimulation, level functions provide a convenient summary of the foregoing results (Fig. 3). Under control conditions the sensitivity displayed compressive nonlinearity at sound-pressure levels exceeding 60 dB. After

anoxia, in contrast, the sensitivity declined and depended linearly on the strength of stimulation. The separation between the data for these two conditions reflects the gain of the active process at each stimulus level. Both amplification and compressive nonlinearity disappeared when we blocked somatic motility, active hair-bundle motility, or both (Fig. 3a-c). The application of Ca^{2+}, Rp-cAMPS, or 8-Br-cAMP produced distinct effects: although these treatments dramatically reduced compressive nonlinearity, a substantial amount of amplification persisted in each instance (Fig. 3d-f).

Discussion

Near the peak of a traveling wave, the active process of a healthy cochlea strongly amplifies weak inputs but provides progressively less enhancement of stronger signals. This level-dependent amplification underlies the cochlea's signature compressive nonlinearity. Here we have shown that perturbing active hair-bundle motility linearizes the basilar membrane's response to sound but spares significant amplification. How can this behavior be understood?

Dynamical systems theory provides useful insight into the results. In this mathematical framework the cochlea's nonlinear responsiveness signifies operation near a bifurcation; the association of frequency tuning with amplification suggests the involvement of a supercritical Hopf bifurcation in particular[29-34]. Consider a system that is stimulated by a sinusoidal pressure of amplitude $\tilde{p}$ at an angular frequency ω. Assume that the pressure acts on a segment of the basilar membrane of area A to produce a force $A\tilde{p}$. The normal form of a Hopf bifurcation with forcing captures the essential features of the system's temporal evolution:

$$\lambda \frac{\partial z}{\partial t} = (a + i\omega_0 \lambda) z - b|z|^2 z + A\tilde{p}e^{i\omega t}, \qquad (1)$$

in which λ is a friction coefficient and ω_0 is the system's resonant frequency. The parameter a represents the real component of the system's linear response, which reflects viscous damping and measures the distance from the Hopf bifurcation, which occurs at the critical value a=0. We consider only positive values of a, for which the system is quiescent in the absence of external

stimulation. The parameter *b* controls the nonlinearity; its real part is positive for a supercritical Hopf bifurcation. As a simplification, we assume that *b* is real.

Acoustic stimulation oscillates the basilar membrane at the same frequency, evoking a displacement of complex amplitude $\tilde{X}$: $z = \tilde{X}e^{i\omega t}$. When the stimulus frequency ω equals the system's resonant frequency ω_0, the response satisfies the relation

$$A\tilde{p} = -a\tilde{X} + b\left|\tilde{X}\right|^2 \tilde{X}. \qquad (2)$$

Two distinct regimes emerge for the system's sensitivity. For pressures smaller than a crossover value $p_* = A^{-1}\sqrt{a^3 b^{-1}}$ the resulting displacement grows linearly with the stimulus, $\tilde{X} = -A\tilde{p}/a$. The sensitivity *S*, the ratio of the velocity to the sound-pressure level, is therefore constant at $S = \omega A/a$ (Fig. 4a). In contrast, larger pressures $\tilde{p} >> p_*$ produce a nonlinear displacement, $\tilde{X} = \left(A\tilde{p}/b\right)^{1/3}$; the sensitivity is then nonlinear as well: $S = \omega A^{1/3} b^{-1/3} \tilde{p}^{-2/3}$. Note in particular that the sensitivity declines with increasing sound-pressure level with a slope in logarithmic coordinates of -2/3 (Fig. 4a). The crossover pressure $\tilde{p} >> p_*$ monotonically increases with larger values of *a*; deviating from the Hopf bifurcation accordingly broadens the regime of linear responsiveness. For a system at the Hopf bifurcation, *a*=0, the crossover pressure p_* vanishes and the system's response becomes entirely nonlinear.

This generic behavior can explain our experimental findings. Using realistic values for the parameters *a* and *b* we find that the sensitivity is nonlinear except for low sound-pressure levels (Fig. 4b), as observed for the interferometric data under control conditions. The damping parameter *a* has a small value because forces from outer hair cells counter the hydrodynamic drag that impedes the cochlear partition's movement and position the partition close to a Hopf bifurcation. When the parameter *a* is increased fivefold, the linear component of the system's response becomes more prominent; the sensitivity accordingly remains linear up to almost 80 dB SPL and is reduced except at high sound-pressure levels (Fig. 4b). The resulting curve resembles those that we have observed experimentally (Fig. 3e,f). Perturbing active hair-bundle motility presumably has the effect of reducing the gain from outer hair cells and positioning the

cochlear partition farther from the Hopf bifurcation. An additional tenfold increase in a, which represents a greater deviation from the Hopf bifurcation, further reduces and diminishes the sensitivity as observed in a passive, anoxic cochlea (Fig. 4b).

Perturbing active hair-bundle motility may also alter the nonlinearity and hence the coefficient b in Equation 1. The nonlinearity in the response of the cochlear partition presumably results from the nonlinear opening probability of the bundle's mechanotransduction channels, which in turn is controlled by active adaptation mechanisms[27]. Interfering with the channels' behavior should therefore affect the nonlinearity. The discussion below Equation 2 informs us that, near a Hopf bifurcation, a reduction of the parameter b does not alter the system's sensitivity to weak stimuli. The crossover pressure p_* above which the system's response becomes nonlinear shifts to higher values, however, so that at high sound-pressure levels the perturbed system exhibits a larger response than the control (Fig. 4b). We have observed similar behavior in our experiments (Fig. 3d and Fig. S3).

Our results reveal that active hair-bundle motility is required for the full range of cochlear amplification and compressive nonlinearity. Disturbing hair-bundle motility yields a linearized response that can be understood through a phenomenological model. Each segment of a healthy cochlear partition presumably operates close to a Hopf bifurcation that yields amplification, frequency tuning, and compressive nonlinearity. Pharmacological perturbation results in deviation from the Hopf bifurcation; the system then exhibits a smaller and more linear response at low sound-pressure levels but retains amplification and nonlinearity for strong stimulation.

Exactly how active hair-bundle motility interacts with somatic motility to implement the cochlear active process remains uncertain. Although modeling has proposed ways in which the two mechanisms can efficiently drive the cochlear partition[35-37], the theoretical approach is limited by the precision to which movements of the ear's many interacting structures have been measured. Moreover, the contributions of the two motile activities may change along the cochlea, for the mechanics at the cochlear apex differs from that at the base[3,4,36]. Understanding the interplay between active hair-bundle motility and somatic motility may require measurement

of the complex motions within the active organ of Corti, perhaps in simplified preparations *in vitro*[22,23] or by optical coherence tomography *in vivo*[38,39].

Methods

Experimental procedures

The study used 59 healthy male chinchillas (*Chinchilla lanigera*) with masses of 0.3-0.5 kg. The techniques of anesthesia, surgery, acoustic stimulation, and interferometric recording have been described[15]. All procedures were approved by the Institutional Animal Care and Use Committee of Rockefeller University.

Perilymphatic and endolymphatic perfusion

Solutions were perfused into the perilymph through the tip of 30-gauge needle placed just above the cochlear fenestra used for interferometric recording. The artificial perilymph consisted of 137 mM NaCl, 5 mM KCl, 12 mM $NaHCO_3$, 2 mM $CaCl_2$, 1 mM $MgCl_2$, 1 mM NaH_2PO_4, and 11 mM **D**-glucose. Perilymph containing either 3 mM salicylate or 150 mM KCl was added at a rate of 0.5 ml/min for 1 min.

Solutions were iontophoretically injected into the endolymph through a small hole, 10 μm in diameter, drilled into the otic capsule. We then inserted a glass electrode containing the solution to be assayed (Fig. S4a,b). To confirm that the electrode's tip was in the scala media, we recorded the endocochlear potential with an extracellular amplifier (EXT-02F, NPI) (Fig. S4c). While monitoring the endocochlear potential, we iontophoretically infused Ca^{2+}, BAPTA, 8-Br-cAMP, or Rp-cAMPS into the endolymph by passing 20 μA of current in 500 ms pulses at 1 s intervals for 3-10 min with a current stimulator (A320, WPI)[40]. Neither inserting an electrode nor injecting current into the scala media affected a traveling wave's sensitivity and phase

(Fig. S5). Even after 10 min of application of a current of 20 μA, traveling waves largely maintained their original gain for the subsequent 30 min (Fig. S6).

We measured active traveling waves in approximately half of the preparations. The low success rate stemmed in part from the invasiveness of the surgical procedure, which often decreased an animal's hearing sensitivity[41]. In addition, drilling a hole on the otic capsule for endolymphatic perfusion sometimes injured the tissue in the lateral cochlear wall and thus reduced the endocochlear potential. Of 32 sensitive cochleae, the traveling waves of 23 exhibited compressive nonlinearity that persisted throughout an experiment; from these, 20 were selected for experiments and three for control measurements.

Estimation of parameter values in the model

A Hopf bifurcation can arise in a simple model of the cochlear partition involving mass, damping, and stiffness[34]. In the following we estimate the coefficients *a* of the linear term and *b* of the nonlinear term in the normal form of the Hopf bifurcation (Equation 1) for a particular position along the partition. The analysis refers to a transverse strip of the basilar membrane whose width is 8 μm, that of one hair cell, and whose length is 200 μm, the approximate radial dimension of the basilar membrane.

The real part *a* of the linear term in Equation 1 corresponds to viscous losses, which are proportional to velocity: $a = \omega\lambda$ with the damping coefficient λ. We have employed an angular frequency $\omega = 2\pi \cdot 10^4$ s^{-1} and a low damping coefficient, λ=10 nN·s·m^{-1}, for an active cochlea.

Nonlinearity results from the dependence on the displacement *X* of the open probability of mechanotransduction channels in the hair bundle:

$$P(X) = \frac{1}{1 + e^{-X/X_0}}. \qquad (3)$$

with a characteristic length $X_0 \approx 10$ nm somewhat smaller than the experimentally measured value[20,21]. According to the gating-spring model of hair-bundle mechanics[21,42], the opening and closing of mechanotransduction channels is associated with a force $AP(X)$ that is proportional

to the open probability with a coefficient $A \approx 1$ nN. For small displacements around a resting value X_0=0 the leading nonlinearity of the gating force is cubic and reads $\left(\frac{A}{6}\right)\left.\frac{d^3P(X)}{dX^3}\right|_{X_0=0} X^3$. The coefficient *b* in Equation 1 may accordingly be estimated as $b = \left(\frac{A}{6}\right)\left.\frac{d^3P(X)}{dX^3}\right|_{X_0=0}$.

Acknowledgments: We thank B. Fabella for computer programming and the members of our research group for their critical reading of the text. F. N. was supported by a Postdoctoral Fellowship for Research Abroad from the Japan Society for the Promotion of Science, T. R. by a Career Award at the Scientific Interface from the Burroughs Wellcome Fund, and J. A. N. F. by a Bristol-Myers Squibb Postdoctoral Fellowship in Basic Neurosciences and a research grant from the American Hearing Research Foundation. A. J. H. is an Investigator of Howard Hughes Medical Institute.

References

1. Von Békésy G (1960) *Experiments in Hearing* (McGraw-Hill, New York)
2. Lighthill J (1981) Energy-Flow in the Cochlea. *J Fluid Mech* **106**, 149-213.
3. Ulfendahl M (1997) Mechanical responses of the mammalian cochlea. *Prog Neurobiol* **53**, 331-380.
4. Robles L, Ruggero MA (2001) Mechanics of the mammalian cochlea. *Physiol Rev* **81**, 1305-1352.
5. Gold T (1948) Hearing. II. The Physical Basis of the Action of the Cochlea. *Proc R Soc B* **135**, 492-498.
6. de Boer E (1983) No sharpening? a challenge for cochlear mechanics. *J Acoust Soc Am* **73**, 567-573.
7. Reichenbach T, Hudspeth AJ (2010) Dual contribution to amplification in the mammalian inner ear. *Phys Rev Lett* **105**, 118102.

8. Brownell WE, Bader CR, Bertrand D, de Ribaupierre Y (1985) Evoked mechanical responses of isolated cochlear outer hair cells. *Science* **227**, 194-196.
9. Ashmore J (2008) Cochlear outer hair cell motility. *Physiol Rev* **88**, 173-210.
10. Zheng J, *et al.* (2000) Prestin is the motor protein of cochlear outer hair cells. *Nature* **405**, 149-155.
11. Liberman MC, *et al.* (2002) Prestin is required for electromotility of the outer hair cell and for the cochlear amplifier. *Nature* **419**, 300-304.
12. Cheatham MA, Huynh KH, Gao J, Zuo J, Dallos P (2004) Cochlear function in Prestin knockout mice. *J Physiol (Lond)* **560**, 821-830.
13. Mellado Lagarde MM, Drexl M, Lukashkina VA, Lukashkin AN, Russell IJ (2008) Outer hair cell somatic, not hair bundle, motility is the basis of the cochlear amplifier. *Nat Neurosci* **11**, 746-748.
14. Dallos P, *et al.* (2008) Prestin-based outer hair cell motility is necessary for mammalian cochlear amplification. *Neuron* **58**, 333-339.
15. Fisher JAN, Nin F, Reichenbach T, Uthaiah RC, Hudspeth AJ (2012) The spatial pattern of cochlear amplification. *Neuron*, in press .
16. Martin P, Mehta AD, Hudspeth AJ (2000) Negative hair-bundle stiffness betrays a mechanism for mechanical amplification by the hair cell. *Proc Natl Acad Sci USA* **97**, 12026-12031.
17. Martin P, Hudspeth AJ (2001) Compressive nonlinearity in the hair bundle's active response to mechanical stimulation. *Proc Natl Acad Sci USA* **98**, 14386-14391.
18. Hudspeth AJ (1989) How the ear's works work. *Nature* **341**, 397-404.
19. Fettiplace R, Ricci AJ, Hackney CM (2001) Clues to the cochlear amplifier from the turtle ear. *Trends Neurosci* **24**, 169-175.
20. Kennedy HJ, Evans MG, Crawford AC, Fettiplace R (2003) Fast adaptation of mechanoelectrical transducer channels in mammalian cochlear hair cells. *Nat Neurosci* **6**, 832-836.

21. Kennedy HJ, Crawford AC, Fettiplace R (2005) Force generation by mammalian hair bundles supports a role in cochlear amplification. *Nature* **433**, 880-883.
22. Chan DK, Hudspeth AJ (2005) Ca^{2+} current-driven nonlinear amplification by the mammalian cochlea in vitro. *Nat Neurosci* **8**, 149-155.
23. Chan DK, Hudspeth AJ (2005) Mechanical responses of the organ of corti to acoustic and electrical stimulation in vitro. *Biophys J* **89**, 4382-4395.
24. Kakehata S, Santos-Sacchi J (1996) Effects of salicylate and lanthanides on outer hair cell motility and associated gating charge. *J Neurosci* **16**, 4881-4889.
25. Santos-Sacchi J, Song L, Zheng J, Nuttall AL (2006) Control of mammalian cochlear amplification by chloride anions. *J Neurosci* **26**, 3992-3998.
26. Corey DP, Hudspeth AJ (1983) Kinetics of the receptor current in bullfrog saccular hair cells. *J Neurosci* **3**, 962-976.
27. Martin P, Bozovic D, Choe Y, Hudspeth AJ (2003) Spontaneous oscillation by hair bundles of the bullfrog's sacculus. *J Neurosci* **23**, 4533-4548.
28. Ricci AJ, Fettiplace R (1997) The effects of calcium buffering and cyclic AMP on mechano-electrical transduction in turtle auditory hair cells. *J Physiol (Lond)* **501**, 111-124.
29. Choe Y, Magnasco MO, Hudspeth AJ (1998) A model for amplification of hair-bundle motion by cyclical binding of Ca^{2+} to mechanoelectrical-transduction channels. *Proc Natl Acad Sci USA* **95**, 15321-15326.
30. Camalet S, Duke T, Julicher F, Prost J (2000) Auditory sensitivity provided by self-tuned critical oscillations of hair cells. *Proc Natl Acad Sci USA* **97**, 3183-3188.
31. Magnasco MO (2003) A wave traveling over a Hopf instability shapes the Cochlear tuning curve. *Phys Rev Lett* **90**, 058101.
32. Duke T, Julicher F (2003) Active traveling wave in the cochlea. *Phys Rev Lett* **90**, 158101.
33. Hudspeth AJ (2008) Making an effort to listen: mechanical amplification in the ear. *Neuron* **59**, 530-545.
34. Hudspeth AJ, Julicher F, Martin P (2010) A critique of the critical cochlea: Hopf—a

bifurcation—is better than none. *J Neurophysiol* **104**, 1219-1229.

35. Ó Maoileidigh D, Julicher F (2010) The interplay between active hair bundle motility and electromotility in the cochlea. *J Acoust Soc Am* **128**, 1175-1190.
36. Reichenbach T, Hudspeth AJ (2010) A ratchet mechanism for amplification in low-frequency mammalian hearing. *Proc Natl Acad Sci USA* **107**, 4973-4978.
37. Meaud J, Grosh K (2011) Coupling active hair bundle mechanics, fast adaptation, and somatic motility in a cochlear model. *Biophys J* **100**, 2576-2585.
38. Chen F, *et al.* (2011) A differentially amplified motion in the ear for near-threshold sound detection. *Nat Neurosci* **14**, 770-774.
39. Zha D, *et al.* (2012) In vivo outer hair cell length changes expose the active process in the cochlea. *PloS ONE* **7**, e32757.
40. Tanaka Y, Asanuma A, Yanagisawa K (1980) Potentials of outer hair cells and their membrane properties in cationic environments. *Hear Res* **2**, 431-438.
41. Ren T, He W, Gillespie PG (2011) Measurement of cochlear power gain in the sensitive gerbil ear. *Nat Commun* **2**, 216.
42. Kennedy HJ, Evans MG, Crawford AC, Fettiplace R (2006) Depolarization of cochlear outer hair cells evokes active hair bundle motion by two mechanisms. *J Neurosci* **26**, 2757-2766.

Figure legends

Figure 1. Characteristics of the traveling wave on the chinchilla's basilar membrane. **a,** Schematic illustrations depict the cochlear traveling wave under control conditions (upper panel) and after anoxia (lower panel). In each diagram the black line shows the instantaneous position of the traveling wave on the basilar membrane and the shaded area represents the envelope through a complete cycle of oscillation. **b,** Interferometric measurements indicate the velocities of basilar-membrane oscillation in response to pure-tone stimulation at 9 kHz. The convergence of the curves toward their peaks indicates that the traveling waves under control conditions (upper panel) are compressive at stimulus levels exceeding 40 dB SPL. In contrast, the velocities measured after anoxia (lower panel) scale linearly with sound pressure and the peaks are shifted basally. The results are plotted in 10 dB decrements in sound-pressure level (SPL) from 90 dB to 40 dB. In this and subsequent illustrations, levels are arranged in a chromatic sequence and the cochlear base lies to the left. **c,** Dividing the velocities by the stimulus pressures yields sensitivity measurements. Because the active process is most effective during weak stimulation, the sensitivities are greatest at low sound-pressure levels (upper panel). In the absence of the active process, the sensitivity curves of an anoxic preparation are superimposed (lower panel). In this and subsequent illustrations, pale red shading indicates the entire range of sensitivities under control conditions and pale gray shading shows that after anoxia.

Figure 2. **Effects of interference with active hair-bundle motility and somatic motility.** The responses to sound-pressure levels from 90 dB to 40 dB are arranged in a chromatic sequence; pale blue shading highlights the range of sensitivities after treatment. **a,** After 15 min of perfusion into the perilymph of the scala tympani, 3 mM salicylate reduced the sensitivity to the level characteristic of anoxia. **b,** Following 60 min of endolymphatic iontophoresis, BAPTA likewise lowered sensitivity to the anoxic level. **c,** Perilymphatic perfusion of 150 mM KCl, which affects both active hair-bundle motility and somatic motility, reduced the sensitivity to that

after anoxia. The peaks of the traveling waves in **a-c**, which are indicated in each panel by arrowheads, shifted basally after each treatment to resemble those after anoxia. **d,** Endolymphatic iontophoresis of Ca^{2+} moderately reduced the traveling wave's sensitivity and narrowed its range. **e,** Rp-cAMPS, which interferes with the activation of protein kinase A, reduced the sensitivity of basilar-membrane oscillation. **f,** 8-Br-cAMP, a lipid-soluble analog of cAMP that promotes protein phosphorylation, also diminished the sensitivity. In **d-f** the peaks of the traveling waves moved basally to a lesser extent and broadened less than during anoxia. Note the different abscissa scales, which reflect the sizes of the apertures through which the interferometric measurements were made.

Figure 3. **Analysis of amplification and nonlinear compression.** Level functions relate the sensitivity of traveling-wave responses at a particular location on the basilar membrane to the strength of stimulation. The control data (red) in each panel demonstrate linear behavior for stimuli below 50-60 dB and compressive nonlinearity at higher levels. The responses after anoxia (black) reveal the behavior of the passive cochlea. The difference between the two sets of curves represents the gain at each level of stimulation, with values up to 100X for weak stimuli. **a,** Perilymphatic perfusion of 3 mM salicylate for 15 min lowered the sensitivity to the level encountered after anoxia. The blue data in this and subsequent panels represent the responses after treatment. **b,** BAPTA iontophoresed into the endolymph eliminated mechanoelectrical transduction and rendered the cochlea passive. **c,** A high K^+ concentration in the perilymph depolarized hair cells, perturbing both active hair-bundle motility and somatic motility, and lowered the sensitivity to the value after anoxia. **d,** Raising the endolymphatic Ca^{2+} concentration by iontophoresis, a procedure meant to partly block transduction channels, desensitized the traveling wave and rendered its behavior linear. A gain of about 10X nonetheless persisted. **e,** Rp-cAMPS reduced the cochlear gain to a similar extent but spared some nonlinearity. **f,** 8-Br-cAMP also reduced both the gain and nonlinearity.

Figure 4. **Generic behavior near a Hopf bifurcation. a,** Two distinct regimes emerge for a system's sensitivity near a Hopf bifurcation. The response is linear below a crossover value p_* of the pressure but becomes nonlinear with an exponent of -2/3 for stronger stimulation. **b,** Simulations based on the normal form of the Hopf bifurcation at a position near the peak of the traveling wave demonstrate behaviors similar to those observed experimentally. Small values of the linear coefficient *a*, which correspond to low viscous damping, lead to predominantly nonlinear behavior (red line) similar to that in control experiments. Increasing the coefficient *a* by a factor of five reduces the sensitivity and renders it constant for most the range of sound-pressure levels (continuous blue line). An additional tenfold increase in *a* reduces the sensitivity to the level observed after anoxia (black line). For the value of *a* used for the continuous blue line, reducing the coefficient *b* that controls the nonlinearity to one-tenth its original value does not change the sensitivity for low sound pressures but increases the sensitivity and enhances linearity at high sound pressures (dashed blue line).

Figure 1:

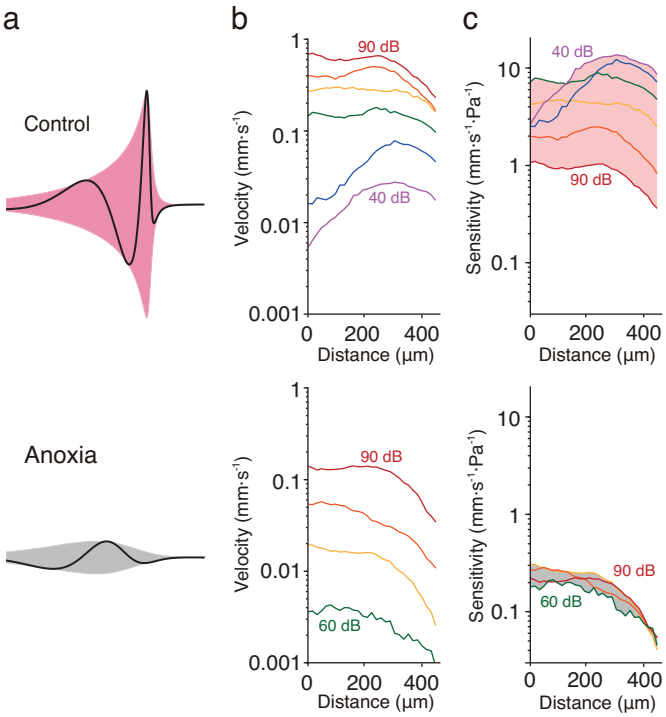
a
b
c
Control
Anoxia
90 dB
40 dB
60 dB
Velocity (mm·s⁻¹)
Sensitivity (mm·s⁻¹·Pa⁻¹)
Distance (µm)
0
200
400
1
0.1
0.01
0.001
10

Figure 2:

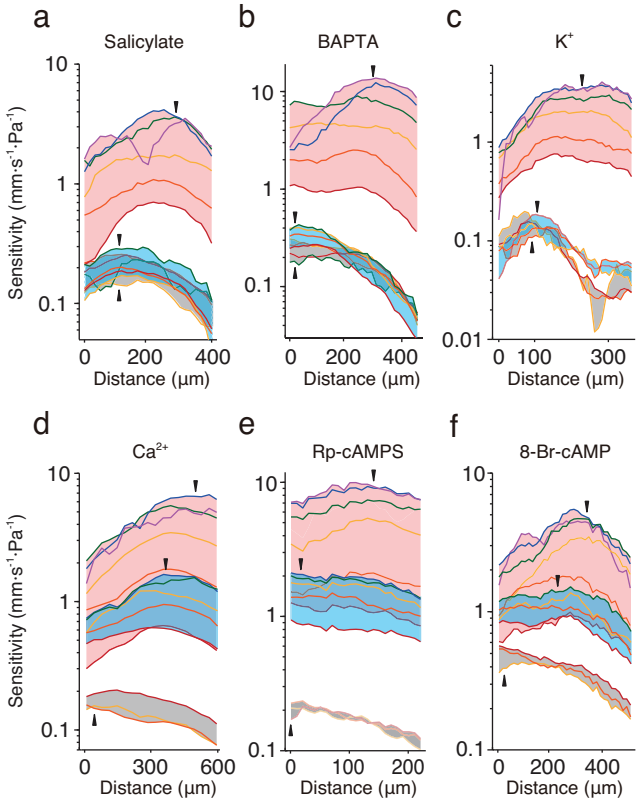
a
Salicylate
b
BAPTA
c
K+
d
Ca2+
e
Rp-cAMPS
f
8-Br-cAMP
Sensitivity (mm·s-1·Pa-1)
Distance (µm)
10
1
0.1
0.01
0
100
200
300
400
600

Figure 3:

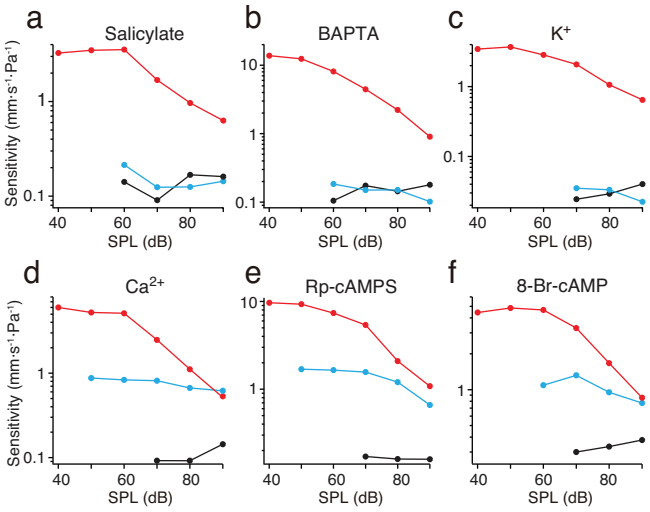
a
Salicylate
b
BAPTA
c
K+
d
Ca2+
e
Rp-cAMPS
f
8-Br-cAMP
Sensitivity (mm·s-1·Pa-1)
SPL (dB)
40
60
80
0.1
1
10

Figure 4:

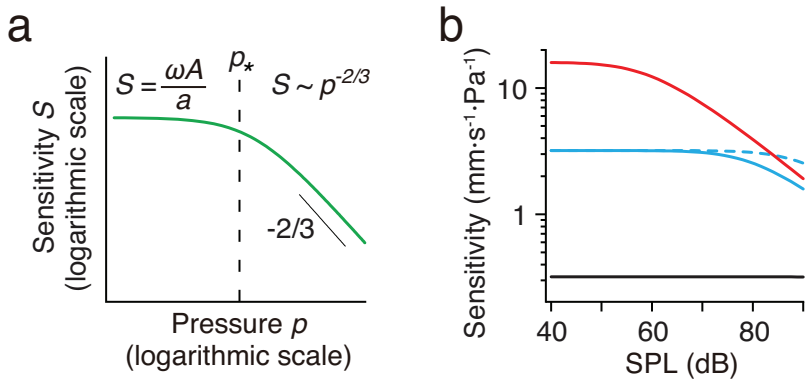
a
$S = \frac{\omega A}{a}$
p_*
$S \sim p^{-2/3}$
-2/3
Sensitivity S
(logarithmic scale)
Pressure p
(logarithmic scale)
b
Sensitivity (mm·s^{-1}·Pa^{-1})
10
1
40
60
80
SPL (dB)